Supporting Information for: Suppression of Auger Recombination in Nanocrystals via Ligand-Assisted Wave Function Engineering in Reciprocal Space

Marco Califano*

Pollard Institute, School of Electronic and Electrical Engineering, University of Leeds, Leeds LS2 9JT, United Kingdom

E-mail: m.califano@leeds.ac.uk

*To whom correspondence should be addressed

Model Ligand Parameters

As the electronic structure calculations are performed in reciprocal space, Eq. (1) needs to be Fourier transformed into[1]

$$v(\mathbf{q}) = \alpha\pi^{1.5}\sigma^3 e^{i\mathbf{q}\cdot\mathbf{R}} e^{-(\sigma|\mathbf{q}|/2)^2} \tag{S1}$$

to obtain the relationship between real-space parameters and q-space ones (which are the actual input to the calculations): $a = \alpha\pi^{1.5}\sigma^3$, $b = \sigma/2$, and $c = \gamma$.

Table S 1: Model ligand parameters used to passivate surface Ga atoms. The parameters relative to the anion passivation [$a_1 = -1$, $b_1 = 0.7$, $c_1 = 0.2$, $a_2 = -1$, $b_2 = 0.9$, $c_2 = 0.2$, where the subscript refers to the number of dangling bonds] were kept constant for all ligands.

Ligand	cation					
	1 dangling bond†			2 dangling bonds†		
	a	b	c	a	b	c
A	2.00	0.1	0.70	2.00	0.50	0.60
B	1.68	0.8	0.55	1.68	0.33	0.25
C	3.00	0.8	0.55	1.68	0.33	0.25
D	3.00	0.8	0.55	4.00	0.33	0.25
E	3.00	0.8	0.45	6.00	0.33	0.25
F	3.00	0.8	0.35	1.68	0.33	0.25

† Surface atoms may have one or two dangling bonds that need passivating (see main text for details)

Method

The single-particle energies and wave functions (E_v, ψ_v and E_c, ψ_c for valence (v) and conduction (c) bands, respectively) are calculated using the plane-wave atomistic semiempirical pseudopotential method described in Reference,[2] including spin-orbit coupling (we use the GaSb pseudopotentials derived by Magri and Zunger[3]).

The reciprocal space decomposition of the CBM is obtained by expanding its wave function $\psi_{cbm}(\vec{r})$ as a superposition of bulk Bloch states $u_{n,\vec{k}}(\vec{r})e^{i\vec{k}\cdot\vec{r}}$ and summing over al bands at a given wave vector $\vec{k}$[4]

$$P_{cbm}(\vec{k}) = \sum_{n=1}^{N_{bands}} \left| \langle \psi_{cbm}(\vec{r}) | u_{n,\vec{k}}(\vec{r}) e^{i\vec{k}\cdot\vec{r}} \rangle \right|^2 \tag{S2}$$

The contributions $c_{\vec{k}}$ from the high-symmetry points (HSP) Γ, L and X are calculated by summing $P_{cbm}(\vec{k})$ over all k points within a Voronoi cell V_{HSP} centred on the specific HSP,[5] as

$$c_{HSP} = 100 \sum_{\vec{k} \in V_{HSP}} P_{cbm}(\vec{k}), \tag{S3}$$

(where HSP=Γ, L or X).

The radiative lifetime for the transition $a \rightarrow b$ are obtained in the framework of the standard time-dependent perturbation theory as:[10]

$$\left(\frac{1}{\tau_R}\right)_{a,b} = \frac{4nF\alpha'\omega^3}{3c^2} |M_{a,b}|^2 \tag{S4}$$

where n is the refractive index of the medium surrounding the nanocrystal (here we assume toluene), $F = 3\epsilon/(\epsilon_{NQD} + 2\epsilon)$ is the screening factor (here $\epsilon = n^2$, and ϵ_{NQD} is the size-dependent dielectric constant of the NQD, calculated using a modified Penn model[11]), α' is the fine structure constant, $\hbar\omega$ is the energy of the photon, c is the speed of light in the vacuum, and $M_{a,b}$ is the excitonic dipole matrix element

$$M_{a,b} = \sum_{v,c} C_{v,c}^{(a)} C_{v,c}^{(b)} \langle \psi_v | \vec{r} | \psi_c \rangle, \tag{S5}$$

where the excitonic wave functions $\{\Psi^{(\beta)}\}$ are expanded in terms of single-substitution Slater determinants $\{\Phi_{v,c}\}$ constructed from the single-particle conduction (c) and valence (v) wave functions and the many-body Hamiltonian is solved within the framework of the Configuration Interaction (CI) scheme, where we use a position-dependent screening for the direct and exchange Coulomb integrals.[11] Room temperature thermally averaged lifetimes are calculated by assuming Boltzmann occupation of the excitonic levels.

Auger recombination rates were calculated within the standard time-dependent perturbation theory according to the formalism developed in ref.[12] following the procedure detailed in ref.,[13] where in the regional screening used in the calculation of the AR integrals a value of 2.4 (toluene) was assumed for the dielectric constant outside the dot and a Lorentzian broadening of 10 meV was used.

Charge Density Profile

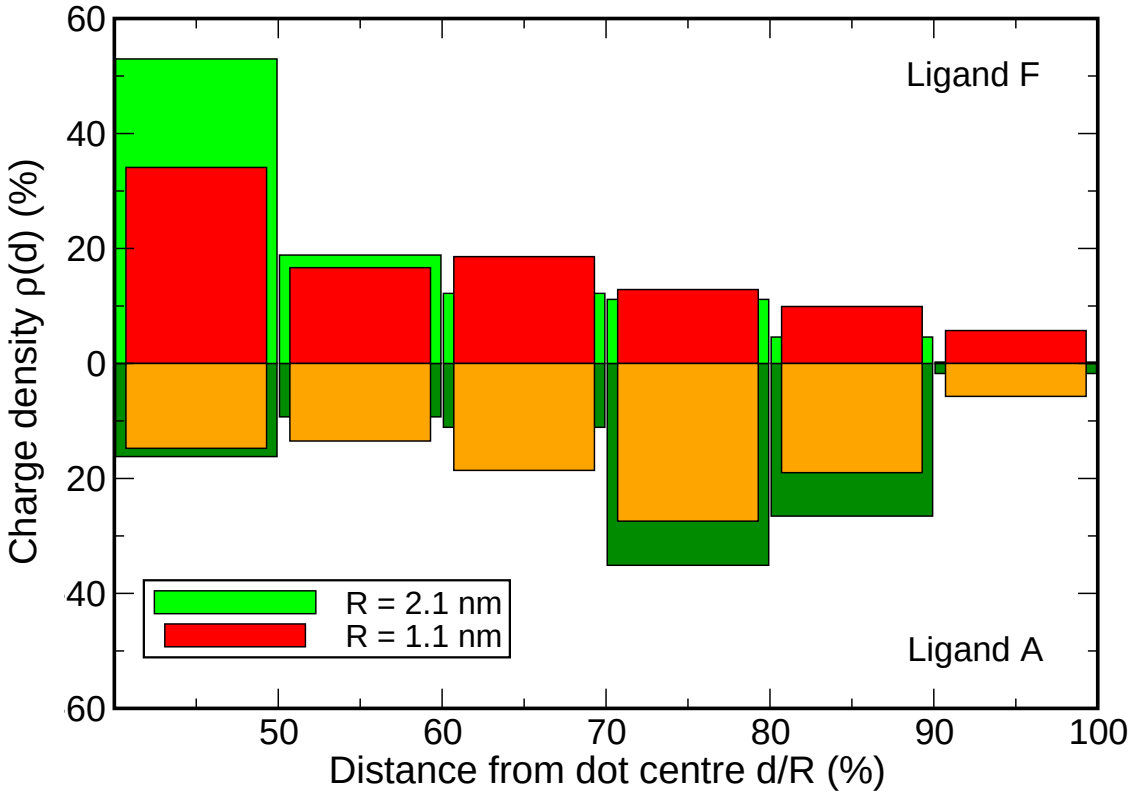

S 1: Charge density profiles for NQDs capped with ligands A and F: charge density contained in equally spaced regions (spherical shells) at different distances d from the nanocrystal centre (expressed as fractions of the total radius R): the first bar refers to the charge density contained in a sphere with radius $r = R/2$ (i.e., $d \leq 50\%$R - the value reported in Fig. 2); the following bars show the density contained in 5 equally spaced spherical shells of width 0.1R, with inner radii ranging from 50%R to 90%R and outer radii from 60%R to 100%R. It is apparent that ligand F leads to a larger concentration of the charge density in the dot core, with about 70% [50%] of the charge located within a sphere with radius 0.6R for $R = 2.1$ nm [$R = 1.1$ nm], whereas ligand A exhibits a larger attraction for the electron, with about 60% [50%] of the charge located between 0.7R and 0.9R for the same size.

Symmetry of the band edge wave functions and character of the ground state excitonic transitions

We find the CBM envelope function of the $R = 2.1$ nm dot to be a_1 (i.e., s-like) for dots capped with ligands A - D, yielding a total orbital symmetry $a_1 = \Gamma_{1c} \times a_1(s)$, for A, and $a_1 = L_{1c} \times a_1(s)$, for B - D. The VBM envelope is found instead to be s-like only for ligand A, yielding and orbital symmetry $t_2 = \Gamma_{15v} \times a_1(s)$, whereas its symmetry is p-like for all other ligands, with orbital symmetry $t_1 = \Gamma_{15v} \times t_2(p)$). Here Γ_{15v}, Γ_{1c}, and L_{1c} represent the symmetry of the underlying bulk Bloch functions (which transform like t_2, a_1 and a_1, respectively), whereas a_1, t_2, etc. are the envelope functions (which are s-like and p-like). Although we include spin-orbit coupling in our calculations, for simplicity we used here the notation relative to $\Delta_{so} = 0$. In the presence of spin-orbit $\gamma_8(t_2)$, $\gamma_8(t_1)$ and $\gamma_8(e)$ are mixed, so that what we refer to as a state with t_2 symmetry has some smaller t_1 and e component, and the same applies for t_1. Further details on the symmetries in NQDs made of zinc-blende materials can be found in ref.[14]

These symmetries result in specific rules for the optical transitions in these systems, as they alter the allowed/forbidden character of the excitonic states that receive contributions from the band edges.

If the VBM is 2-fold degenerate with an overall $\gamma_{8v}(t_2)$ symmetry and the 2-fold degenerate CBM has an overall $\gamma_{6c}(a_1)$ symmetry, the ground state exciton is 5-fold degenerate and dark. The next exciton derived from the band edges is 3-fold degenerate and bright. If, however, the VBM has an overall $\gamma_{8v}(t_1)$ symmetry, while the CBM is still $\gamma_{6c}(a_1)$, the ground state exciton has instead a dipole-allowed component, yielding a partially allowed, 3-fold degenerate, ground exciton, with a much longer lifetime than a fully allowed, bright exciton. Finally with a $\gamma_{8v}(t_1)$ VBM and a $\gamma_{8c}(t_2)$ CBM, we find a the lowest 100 exciton states to be dark.

Radiative Lifetime

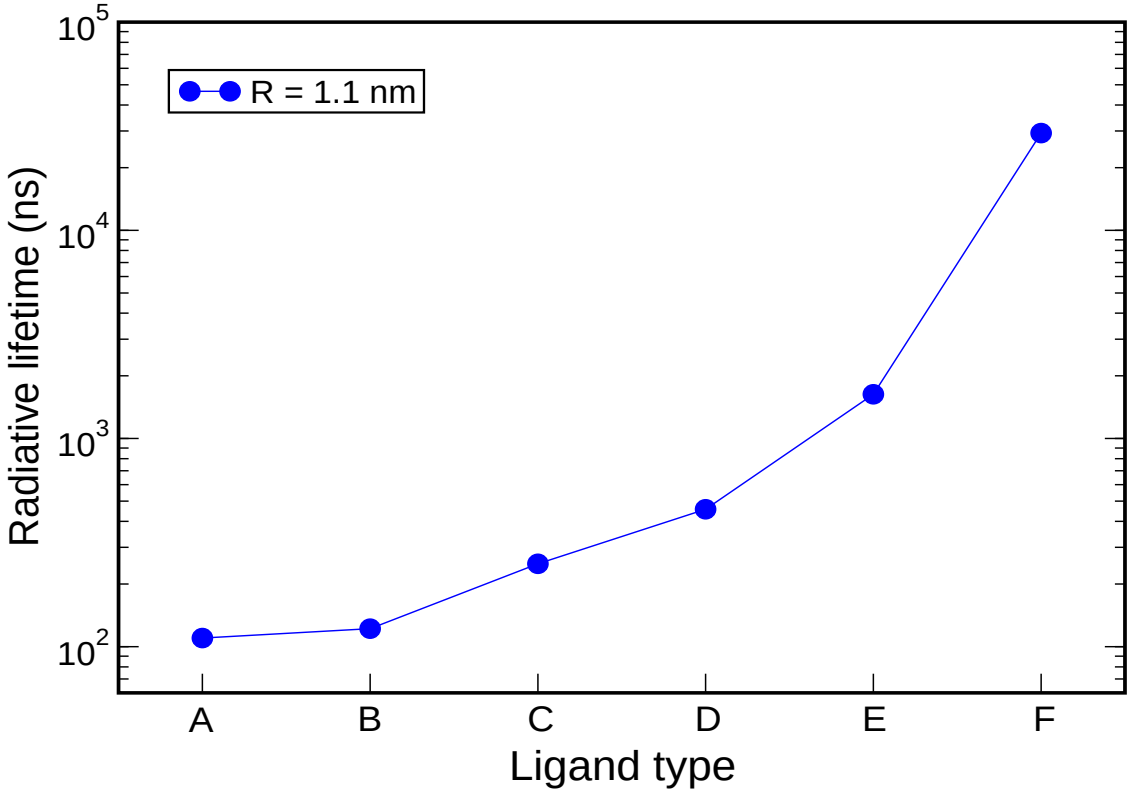

S 2: Radiative lifetimes calculated for NQDs with $R = 1.1$ nm capped with ligands A to F.

Auger Electron Cooling times

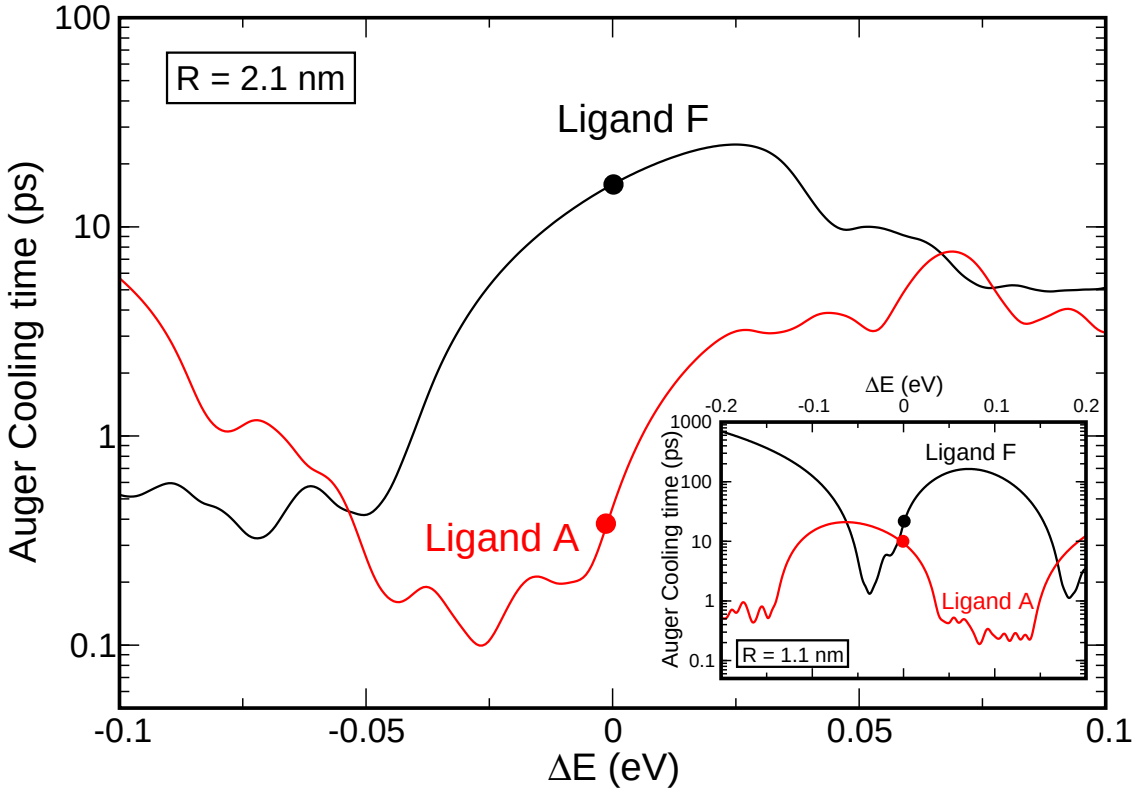

S 3: AC times calculated for NQDs with $R = 2.1$ nm (main frame) and $R = 1.1$ nm (inset) capped with ligands A and F: F-capped nanocrystals exhibit increases in the AC times of over one order of magnitude compared to A-terminated dots, for larger sizes; although at $\Delta E = 0$ the reduction is small (a factor of 2) in $R = 1.1$ nm nanostructures, due to the strongly oscillating character of the results, the AC suppression can approach 3 orders of magnitude in these dots.

References

(1) Graf, P.A.; Kim, K.; Jones, W.B.; Wang, L.W. Surface Passivation Optimization Using DIRECT. *J. Comp. Phys.* **2007**, *224*, 824-835.

(2) Wang, L.-W.; Zunger, A. Local-Density-Derived Semiempirical Pseudopotentials. *Phys. Rev. B* **1995**, *51*, 17 398.

(3) Magri, R.; Zunger, A. Effects of Interfacial Atomic Segregation and Intermixing on the Electronic Properties of InAs/GaSb Superlattices. *Phys. Rev. B* **2002**, *65*, 165302.

(4) Wang, L.-W.; Bellaiche, L.; Wei, S. H.; Zunger, A. "Majority Representation" of Alloy Electronic States. *Phys. Rev. Lett.* **1998**, *80*, 4725.

(5) Following the procedure used in Ref.,[6] the nanocrystal's Brillouin zone was partitioned using the high symmetry points Γ, L and X as seeds for non-overlapping Voronoi cells[7–9] in reciprocal space, having the property that each wave vector k in any particular cell is closer to the specific high-symmetry point than to any other.

(6) Sills, A.; Harrison, P.; Califano, M. Exciton Dynamics in InSb Colloidal Quantum Dots. *J. Phys. Chem. Lett.* **2015** *7*, 31-35

(7) Aurenhammer, F. Voronoi Diagrams - A Survey of a Fundamental Geometric Data Structure. *ACM Computing Surveys* **1991**, *23*, 345-405.

(8) Okabe, A.; Boots, B.; Sugihara, K.; Chiu, S. N. *Spatial Tessellations - Concepts and Applications of Voronoi Diagrams*. 2nd edition. John Wiley, 2000, ISBN 0-471-98635-6.

(9) Tran, Q.T.; Tainar, D.; Safar, M. *Transactions on Large-Scale Data- and Knowledge-Centered Systems*, **2009**, ISBN 9783642037214.

(10) Dexter, D. L. *Solid State Physics* **1958** (Academic Press Inc., New York), vol. *6*, p. 358-361.

(11) Franceschetti, A.; Fu, H.; Wang, L.-W. & Zunger, A. Many-Body Pseudopotential Theory of Excitons in InP and CdSe Quantum Dots. *Phys. Rev. B* **1999**, *60*, 1819-1829.

(12) Wang, L.-W.; Califano, M.; Franceschetti, A.; Zunger, A. Pseudopotential Theory of Auger Processes in CdSe Quantum Dots. *Phys. Rev. Lett.* **2003**, *91*, 056404-1 - 056404-4.

(13) Califano, M. Direct and Inverse Auger Processes in InAs Nanocrystals: Can the Decay Signature of a Trion Be Mistaken for Carrier Multiplication? *ACS Nano* **2009**, *3*, 2706-2714.

(14) Yu, P.Y.; Cardona, M. Fundamentals of Semiconductors: Physics and Materials Properties. 4th edtion. Springer Berlin Heidelberg, **2010**, ISBN 978-3-642-00709-5.